Journal of Photochemistry and Photobiology B: Biology 126 (2013) 78–86

Contents lists available at SciVerse ScienceDirect

Journal of Photochemistry and Photobiology B: Biology

journal homepage: www.elsevier.com/locate/jphotobiol

Zinc(II) complexes of Pro-Gly and Pro-Leu dipeptides: Synthesis, characterization, *in vitro* DNA binding and cleavage studies

Shazia Parveen [a], Farukh Arjmand [a,*], D.K. Mohapatra [b]

[a] Department of Chemistry, Aligarh Muslim University, Aligarh 202 002, India
[b] Diversity Oriented Synthesis Laboratory, Indian Institute of Chemical Technology, Hyderabad 500 607, India

ARTICLE INFO

Article history:
Received 19 February 2013
Received in revised form 10 May 2013
Accepted 7 July 2013
Available online 17 July 2013

Keywords:
Dipeptide complexes
Hydrolytic cleavage
Minor groove
T4 DNA ligase
Molecular docking

ABSTRACT

Dipeptide (Pro-Gly and Pro-Leu) Zinc(II) complexes **1** and **2** were designed and synthesized for potential use as cancer chemotherapeutic agents. In order to augment the DNA recognition of metallonuclease activity, zinc metal ion was tethered to peptide motif to carry out DNA site specific hydrolytic cleavage. The structural formulation of the complexes **1** and **2** was done by elemental analysis, spectroscopic methods (IR, NMR, electronic) and molar conductance measurements. Their *in vitro* DNA binding profile was investigated by UV–vis titrations, fluorescence titrations and circular dichroism which revealed that these complexes bind to CT DNA by electrostatic interactions *via* groove binding mode. Zn(II) Pro-Gly complex **1** showed greater binding affinity to CT DNA as compared to the Zn(II) Pro-Leu complex **2** due to steric constraints in the latter. The supercoiled pBR322 DNA cleavage activity of complex **1**, ascertained by gel electrophoresis demonstrated efficient DNA cleaving ability *via* hydrolytic mechanistic pathway. Further, the molecular docking studies confirmed that complex **1** bind to the minor groove of DNA having AT-rich sequences with relative binding energy of -196.72 kJ mol^{-1}.

1. Introduction

The design of small chemical entities that bind to DNA have attracted much interest towards the development of artificial nucleases [1], antitumor drugs [2] and sensitive chemical probes for mapping nucleic acid structures [3]. Protein and peptide-based artificial nuclease agents are specifically capable of recognizing double-stranded DNA in a manner similar to transcription factors and recognition enzymes [4]. Peptides play important roles as hormones, enzyme inhibitors, neurotransmitters and immunomodulators in living systems and therefore, are expected to play significant role in the treatment of many diseases *viz.*, cancer, AIDS, Alzheimer's disease, malaria and as antimicrobials. Recently, it has been reported that some peptide derivatives show antitumor activity with little toxicity against non-malignant cells either by triggering apoptosis [5] or by forming ion channels/pores [6]. Furthermore, some peptides were found to be cytotoxic against MDR cancer cells [7,8]. Metal–peptide conjugate chemistry offers novel design for the development of artificial nucleases as metal ions can be tuned to cleave DNA in a site selective manner while the peptide have potential to control specific gene expression and is capable to permeate biomembrane easily and transport biologically active component of drugs *in vitro* and *in vivo*, thereby possessing good biological/pharmacological activity [9]. Earlier studies have shown that tethering of small peptides to a metal complex exhibit specific DNA binding capability which was governed by the appended peptide [10].

In lieu of above and in continuation of our previous work [11], we report herein the synthesis and characterization of dipeptide (Pro-Gly/Pro-Leu) Zn(II) complexes and their *in vitro* DNA binding studies. The complex **1** has been developed as hydrolytic pBR322 DNA cleaving agent. Zinc is an ideal metal ion to be explored as a hydrolytic catalyst owing to its unique chemistry (i) non-redox, (ii) high Lewis acidity (exchange ligands very rapidly) and (iii) plays an important role in phosphodiester cleavage [12].

2. Materials and methods

2.1. Materials

All reagents were of best commercial grade and were used without further purification. L-proline, L-leucine, glycine, HOBT (SRL), EDCI, ascorbic acid, zinc nitrate hexahydrate, (Merck), H_2O_2, 3-mercaptopropionic acid, glutathione, methyl green, DAPI, tertiary butyl alcohol, sodium azide, superoxide dismutase (Sigma), 6X loading dye (Fermentas Life Science) and Supercoiled plasmid pBR322 DNA (Genei) were utilized as received. CT DNA was purchased from Sigma Chemical Co. and were stored at 4 °C.

* Corresponding author. Tel.: +91 5712703893.
E-mail address: farukh_arjmand@yahoo.co.in (F. Arjmand).

1011-1344/$ - see front matter © 2013 Elsevier B.V. All rights reserved.
http://dx.doi.org/10.1016/j.jphotobiol.2013.07.009

2.2. Characterization

The energy minimized 3-dimensional molecular structures of complexes **1** and **2** are represented in Fig. 1. Infrared spectra were recorded on Interspec 2020 FTIR spectrometer in KBr pellets from 400 to 4000 cm^{-1}. The elemental analyses were performed on Carlo Erba analyzer model 1106. The NMR spectra were obtained on a Bruker DRX-400 spectrometer operating at room temperature. Electrospray mass spectra were recorded on Micromass Quattro II triple quadrupol mass spectrometer. XRD were recorded on Rikagu mini Flex II Instrument. Electronic spectra were recorded on a UV-1700 PharmaSpec UV-vis Spectrophotometer. Fluorescence measurements were made on Hitachi F-2500 fluorescence spectrophotometer. Molar conductance was measured at room temperature on Eutech con 510 electronic conductivity bridge. CD spectra were recorded on Applied Photophysics Chirascan Circular Dichroism Spectrometer with Stop Flow. While measuring the absorption spectra an equal amount of DNA was added to both the compound solution and the reference solution to eliminate the absorbance of the CT DNA itself, and the CD contribution by the CT DNA and Tris buffer was subtracted through base line correction.

2.3. DNA binding and cleavage experiments

DNA binding experiments which include absorption spectral traces, emission spectroscopy and circular dichroism conformed to the standard methods and practices previously adopted [13–16]. DNA cleavage experiment has been performed by the standard protocol [17,18].

2.4. Molecular docking studies

The rigid molecular docking studies were performed by using HEX 6.3 software, [19] is an interactive molecular graphics program to understand the drug–DNA interactions. The Structure of the complex was sketched by CHEMSKETCH (http://www.acdlabs.com) and converted to pdb format from mol format by OPENBABEL (http://www.vcclab.org/lab/babel/). The crystal structure of the B-DNA dodecamer $d(CGCGAATTCGCG)_2$ (PDB ID: 1BNA) was downloaded from the protein data bank (http://www.rcsb.org./pdb). All calculations were carried out on an Intel pentium4, 2.4 GHz based machine running MS Windows XP SP2 as operating system. Visualization of the docked pose has been done by using CHIMERA (http://www.cgl.ucsf.edu/chimera/) molecular graphics program.

2.5. Synthesis

2.5.1. Protection of terminal groups of amino acids

2.5.1.1. Protection of terminal amino group of amino acid (Boc-protection of L-Gly/L-Leu). To a stirred solution of NaOH (2.5 M) in H_2O-dioxane (1:1) mixture, L-glycine (0.75 g, 10 mmol)/L-leucine (1.31 g, 10 mmol) was added. To this, Boc anhydride (2.62 g, 10 mmol) was added drop wise and stirred for 6 h at room temperature to give a white precipitate. Dioxane was removed under reduced pressure, acidified with $KHSO_4$ upto pH 3 on ice bath. The organic layer was dried over anhydrous Na_2SO_4 and evaporated under reduced pressure to give the crude product which was finally purified by column chromatography.

2.5.1.2. Protection of terminal carboxyl of amino acid (Ester protection of L-Pro): By esterification with MeOH/$SOCl_2$. To a stirred solution of L-proline (1.15 g, 10 mmol) in methanol (30 mL), $SOCl_2$ (2.86 mL, 40 mmol) was added drop wise at 0 °C under inert atmosphere and refluxed at 70 °C for 3–4 h. The progress of the reaction was monitored by TLC. On completion of the reaction the solvent was removed under reduced pressure to give yellow colored oil of L-proline methyl ester hydrochloride.

2.5.2. Synthesis of dipeptide ligands, Pro-Gly and Pro-Leu

The dipeptide ligands were synthesised following the solution phase peptide synthesis [20] (Scheme 1).

Dry dichloromethane (DCM, 20 mL) was added to Boc-gly-OH (1.75 g, 10 mmol)/Boc-Leu-OH (2.31 g, 10 mmol) under inert atmosphere. To this solution, EDCI (4.77 g, 25 mmol) was added at 0 °C and the reaction mixture was stirred for 20 min. Pro-OMe (1.29 g, 10 mmol) was added followed by HOBT (2.74 g, 20 mmol) to the above reaction mixture under stirring and the reaction was continued for 12 h. On completion of the reaction, it was monitored by TLC using EtOAc. For detection a solution of ninhydrin was used. The reaction mixture was filtered to remove white precipitate. The residue was washed with DCM (30 mL) and added to the filtrate. The filtrate was washed with 5% sodium bicarbonate and saturated sodium chloride solutions. The organic layer was dried over anhydrous Na_2SO_4, filtered and evaporated under reduced pressure. The crude product was purified by column chromatography (15% acetone and hexane mixture).

2.5.2.1. Pro-Gly. Yield: 62%, Anal. Calc. for $C_{13}H_{22}N_2O_5$ (%) C, 54.53; H, 7.74; N, 9.78. Found: C, 54.78; H, 7.92; N, 10.12. Selected IR data (KBr, cm^{-1}); 2885 $\nu(O—H)_{carbonyl}$, 1710 $\nu(CO)_{pep}$ amide I, 1654 ν_{as} (COO), 1364 ν_s(COO). ^1H NMR (300 MHz, $CDCl_3$, δ ppm): 5.4 (1H, NH_{Boc}), 4.5 (t, 1H, chiral pro CH), 3.9 (s, 2H, gly-CH_2), 3.7 (s, 3H, O—CH_3 ester H), 3.6 (t, 2H, pro-CH), 2.2–2.4 (m, 4H, pro-CH_2), 1.4

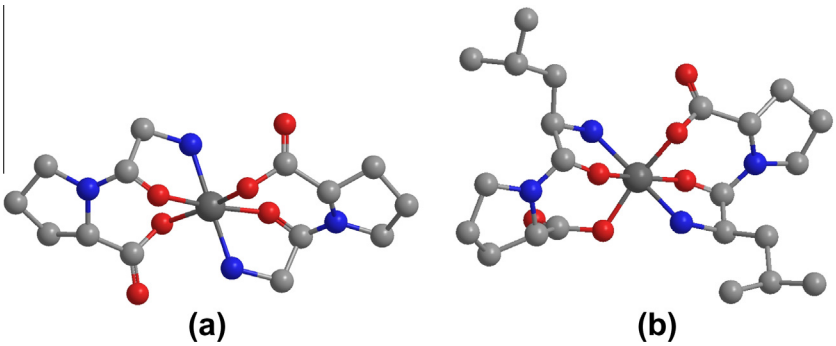

Fig. 1. The energy minimized cylindrical bonded 3-dimensional molecular structures of complexes (a) **1** and (b) **2**. Color scheme: Nitrogen (blue), oxygen (red) Zn(II) (dark grey) and carbon (grey). Hydrogen atoms have been omitted for clarity. (For interpretation of the references to color in this figure legend, the reader is referred to the web version of this article.)

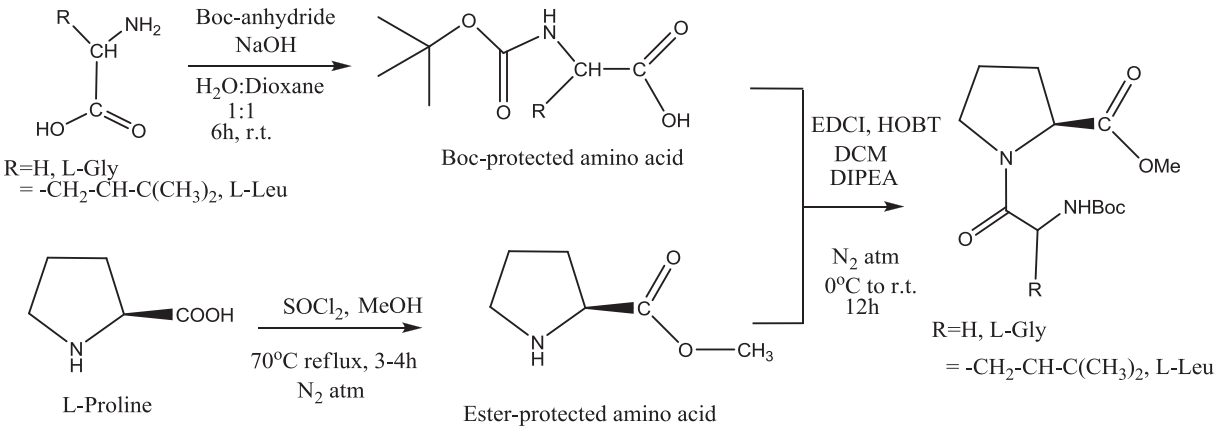

Scheme 1. Schematic representation of the synthesis of dipeptide ligands Pro-Gly and Pro-Leu.

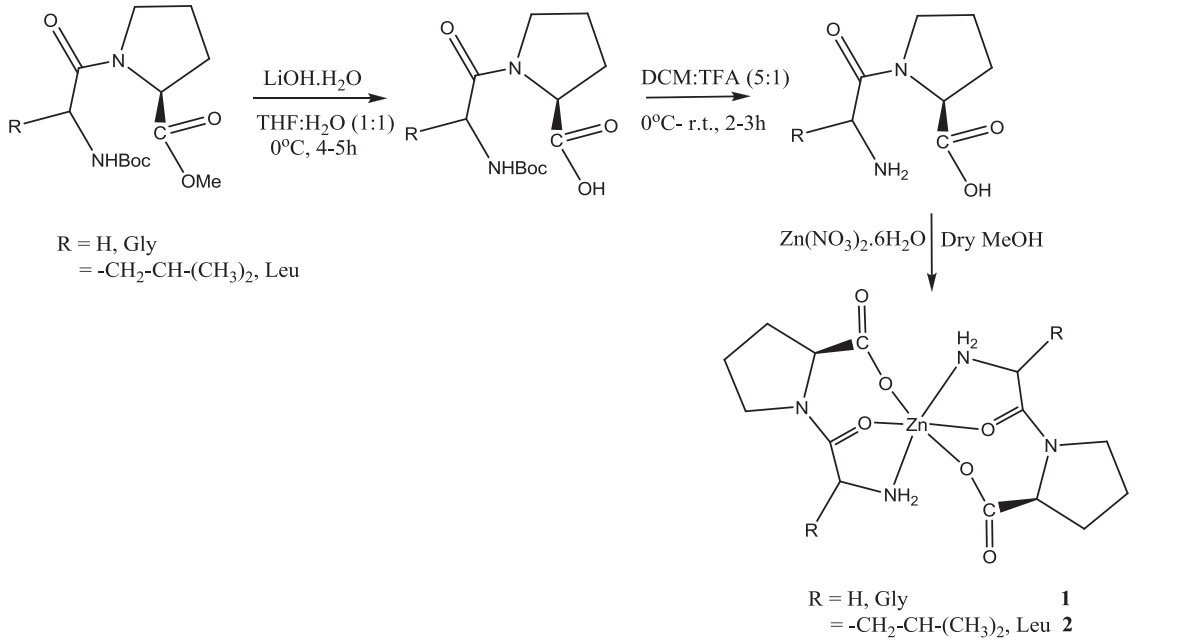

Scheme 2. Synthesis of dipeptide Zn(II) complexes **1** and **2**.

(s, 9H, Boc protons). ^{13}C NMR (300 MHz, $CDCl_3$, δ ppm): 172 (C═O_{pep} carbonyl), 167 (C═O ester carbonyl), 155 (C═O, Boc carbonyl C), 58.8 (pro chiral C), 52.3 (ester C), 45.8 (2C, gly CH_2), 42.9 (1C, pro-CH_2), 28.9 (3C, Boc-C), 24 (2C, pro C). UV–vis (10^{-4} M, MeOH, nm): 225.2, 283.2. $[\alpha]_D$ (MeOH), −56.9. ESI (m/z^+), 287 [$C_{13}H_{22}N_2O_5 + H^+$].

2.5.2.2. Pro-Leu. Yield: 58%, Anal. Calc. for $C_{17}H_{30}N_2O_5$ (%) C, 59.61; H, 8.84; N, 8.18. Found: C, 59.86; H, 8.91; N, 8.79. Selected IR data (KBr, cm^{-1}); 2876 ν(O—H)$_{carbonyl}$ 1705 ν(CO)$_{pep}$ amide I, 1650 ν_{as} (COO), 1366 ν_s(COO). ^{1}H NMR (300 MHz, $CDCl_3$, δ ppm): 5.1 (1H, NH_{Boc}), 4.5 (t, 1H, pro chiral CH), 3.7 (m, chiral Leu CH_2), 3.5 (t, 2H, pro-CH_2), 3.6 (s, 3H, O—CH_3 ester H), 2.1 (m, 4H, pro-CH_2), 1.7 (dd, 2H, Leu-CH_2), 1.4 (s, 9H, Boc protons), 0.98 (6H, Leu CH_3). ^{13}C NMR (300 MHz, $CDCl_3$, δ ppm): 172.4 (C═O_{pep} carbonyl), 171.7 (C═O ester carbonyl), 155.6 (C═O, Boc carbonyl C), 58.6 (pro chiral C), 52.09 (1C, Leu C), 50.21 (ester C), 46.6 (1C, pro CH_2), 41.8 (1C, Leu CH_2), 28.8 (3C, Boc-C), 24 (2C, pro C), 21–23 (2C Leu CH_3 and 1C Leu CH). UV–vis (10^{-4} M, MeOH, nm): 226.6, 282.0. $[\alpha]_D$ (MeOH), −63.8. ESI (m/z^+), 343 [$C_{17}H_{30}N_2O_5 + H^+$].

2.5.3. Deprotection of terminal groups of amino acids

2.5.3.1. Deprotection of ester-protected amino acids: The methyl ester group was removed by alkaline hydrolysis with LiOH. Dried THF:H_2O (1:1) was added to Boc-gly-pro-OMe (2.86 g, 10 mmol)/Boc-Leu-pro-OMe (3.42 g, 10 mmol). To this, lithium hydroxide monohydrate (0.36 g, 15 mmol) was added at 0 °C and stirred for 4–5 h. The product was isolated by adding water, acidifying upto pH 3 with $KHSO_4$ and extracted with EtOAc (3 × 35 mL). The colorless oil was dried under reduced pressure and dried over $NaSO_4$.

2.5.3.2. Deprotection of Boc-protected amino acids: The Boc group was removed by treatment with trifluoroacetic acid. To a stirred solution of Boc-gly-pro-OH (2.72 g, 10 mmol)/Boc-Leu-pro-OH (3.28 g, 10 mmol) in anhydrous DCM, TFA was added slowly at 0 °C (DCM: TFA = 5:1) under inert atmosphere and stirred for 2–3 h. The unreacted TFA was removed under reduced pressure and

resulting solution was diluted with DCM, neutralized with DIPEA or ammonia solution.

*2.5.4. Synthesis of Zn(II) complexes **1** and **2***

To a stirred methanolic solution of deprotected Pro-Gly (0.572 g, 2 mmol)/Pro-Leu (0.684 g, 2 mmol), $Zn(NO_3)_2{\cdot}6H_2O$ (0.297 g, 1 mmol) was added under dry conditions and the resultant solution was stirred for 1 h. The complex precipitated as a white product which was filtered, washed with petroleum ether and dried *in vacuo* (Scheme 2).

*2.5.4.1. [Zn(Pro-Gly)$_2$], **1**.* Yield, 69%. Anal. Calc. for $C_{14}H_{22}N_4O_6Zn$ (%) C, 41.24; H, 5.44; N, 13.74. Found: C, 41.78; H, 5.67; N, 13.92. Selected IR data (KBr, cm^{-1}): 3208 $\nu_{as}(NH_2)$, 3035 $\nu_s(NH_2)$, 1673 $\nu_{as}(COO) + \nu(C{=}O)$ amide I, 1439 $\nu_s(COO)$, 1202 $\delta(NH)$, 454 (Zn–N); 530 (Zn–O). ^{1}H NMR (400 MHz, δ, ppm): 4.33 (t, 2H, chiral pro CH), 3.85 (s, 4H, gly-CH_2), 3.6 (t, 4H, pro-CH), 2.02–2.33 (8H, pro-CH_2). Molar Conductance, Λ_M (10^{-3} M, DMSO): 12.0 Ω^{-1} cm^2 mol^{-1} (non-electrolyte). $[\alpha]_D$ (MeOH), −52.2. UV–vis (10^{-4} M, DMSO, nm, ε, L mol^{-1} cm^{-1}): 227 (7800), 298 (4300). ESI–MS (m/z^+): 407 [$C_{14}H_{22}N_4O_6Zn$].

*2.5.4.2. [Zn(Pro–Leu)$_2$], **2**.* Yield, 71%. Anal. Calc. for $C_{22}H_{38}N_4O_6Zn$ (%) C, 50.94; H, 7.39; N, 10.81. Found: C, 51.26; H, 7.80; N, 11.04. Selected IR data (KBr, cm^{-1}): 3145 $\nu_{as}(NH_2)$, 3032 $\nu_s(NH_2)$, 1653 $\nu_{as}(COO) + \nu(C{=}O)$ amide I, 1400 $\nu_s(COO)$, 1198 $\delta(NH)$, 461 (Zn–N); 522 (Zn–O). ^{1}H NMR (400 MHz, δ, ppm): 4.32 (t, 2H, pro chiral CH), 3.91 (m, chiral Leu CH_2), 3.7 (t, 2H, pro-CH_2), 2.11–2.34 (m, 8H, pro-CH_2), 1.9 (dd, 4H, leu-CH_2), 1.01 (6H, Leu CH_3). Molar Conductance, Λ_M (10^{-3} M, DMSO): 17.0 $\Omega^{-1}cm^2$ mol^{-1} (non-electrolyte). $[\alpha]_D$ (MeOH), −61.1. UV–vis (10^{-4} M, DMSO, nm, ε, L mol^{-1} cm^{-1}): 223 (10,200), 291 (7900). ESI–MS (m/z^+): 519 [$C_{22}H_{38}N_4O_6Zn$].

3. Results and discussion

3.1. Characterization

3.1.1. IR spectroscopy

Non-coordinated peptides, in the IR spectra should exhibit strong absorption bands assigned to ν(N—H) in the range of 3288–3017 cm^{-1} [21] which were absent in free ligands as the terminal amino group was Boc-protected. There was a substantial lowering of the two absorption bands in the region 3204–3030 cm^{-1} assigned to the antisymmetric and symmetric —NH_2 stretching modes [22] indicating the coordination by amino group to the metal ion. The magnitude of the $\nu_{as}(COO)$—$\nu_s(COO)$ ($\Delta\nu$) separation in the complexes **1** and **2** was in the range of 234–253 cm^{-1} suggestive of coordination of the carboxylate group in a monodendate fashion [23]. Further, in the free ligands, a medium intensity band in the region of 2885–2961 cm^{-1} attributed to $\nu(O{-}H)_{carboxyl}$ was disappeared in the spectra of Zn(II) complexes **1** and **2**, suggesting the deprotonation of –COOH group upon complexation [24].

3.1.2. NMR spectroscopy

The ^{1}H NMR spectra of the ligands, Pro-Gly and Pro-Leu revealed singlets of O—CH_3 ester protons and t-Boc protons at 3.6 and 1.4 ppm, respectively, which disappeared upon deprotection of these groups and new signals emerged at 12.0–13.0 ppm corresponding to —COOH group which was absent in the complexes indicating the coordination of carboxylic group to Zn(II) through deprotonation [25]. The NH_2 signal in the complexes could not be resolved as it has possibly merged with the solvent peak at 4.8 ppm due to the rapid proton exchange with the solvent D_2O [26]. The signals at 2.2–2.4 (quintet), 3.5–3.6 (triplet) and 4.5–4.6 (triplet) ppm were attributed to proline moiety in the dipeptide ligands and complexes [27]. While the signal at 3.91 ppm corresponds to the glycine, and the signals at 1.7 (doublet) and 0.9–1.01 ppm were attributed the leucine moiety in the ligands and complexes [25].

3.1.3. Mass spectrometry

The ESI–MS spectra of the ligands displayed prominent peaks at m/z 287 and 343 corresponding to [$C_{13}H_{22}N_2O_5 + H^+$] and [$C_{17}H_{30}N_2O_5 + H^+$], respectively. ESI–MS spectra of the complexes displayed prominent peaks corresponding to the molecular ion fragment. The complexes **1** and **2** displayed prominent peak at m/z 407.0 and 519.2 corresponding to [$C_{14}H_{22}N_4O_6Zn$] and [$C_{22}H_{38}N_4O_6Zn$], respectively.

3.1.4. Electronic absorption spectroscopy

The absorption spectra of the ligands recorded in MeOH at room temperature revealed $n \rightarrow \pi^*$ transitions at 225 nm [28]. The complexes **1** and **2** exhibited (N → M) LMCT transition bands at 223 and 227 nm, respectively. Other medium intensity bands at 298 and 291 nm for complexes **1** and **2**, respectively attributed to ($COO^- \rightarrow M$) charge transfer transitions and were well in agreement with hexa-coordinated environment around the Zn(II) ion [29].

3.1.5. X-ray diffraction analysis

To obtain further evidence about the crystalline nature of complexes **1** and **2**, XRPD studies were performed. The XRPD diffractograms obtained for the complexes **1** and **2** depicted in Fig. 2, indicated their crystalline nature.

3.2. DNA binding studies

DNA binding studies are important for the rational design and construction of new and more efficient drugs targeted to DNA. The biologically relevant B-form of DNA double helix is characterized by a shallow-wide major groove and deep-narrow minor groove. A variety of small molecules interact reversibly with double stranded DNA, primarily through three modes: (i) electrostatic interactions with the negative charged nucleic sugar–phosphate structure, which are along the external DNA double helix and do not possess selectivity; (ii) binding interactions with two grooves of DNA double helix and (iii) intercalation between the stacked base pairs of native DNA [30].

3.2.1. UV–vis absorption titrations

With the increasing amount of CT DNA, the charge transfer bands of the complexes **1** and **2** at ~270–290 nm showed variation in the intensity exhibiting hyperchromism with practically no change in the position of the absorption bands; ruling out intercalative binding of the complexes to DNA (Fig. 3). These results were suggestive of the possibility of groove binding for the complexes to DNA [31]. Groove binders are another major class of molecules that play an important role in drug development. The formation of a DNA–peptide complex can induce changes in the spectral characteristics of both or either of DNA or peptide [32]. Tethering of peptides to metals augment DNA binding affinity. It is likely that the complexes can form hydrogen bonds with N-3 of adenine or O-2 of thymine in the major groove of DNA *via* amine group of peptide moiety, which may contribute to the hyperchromism observed in the absorption spectra. The hydrophobic residues in peptides increase the stability of the peptide–DNA complex [33] and it is more likely that the hydrophobic interactions and the H-bonding ability of the peptide moiety can be responsible for the DNA binding ability of complexes. In order to compare the binding strength

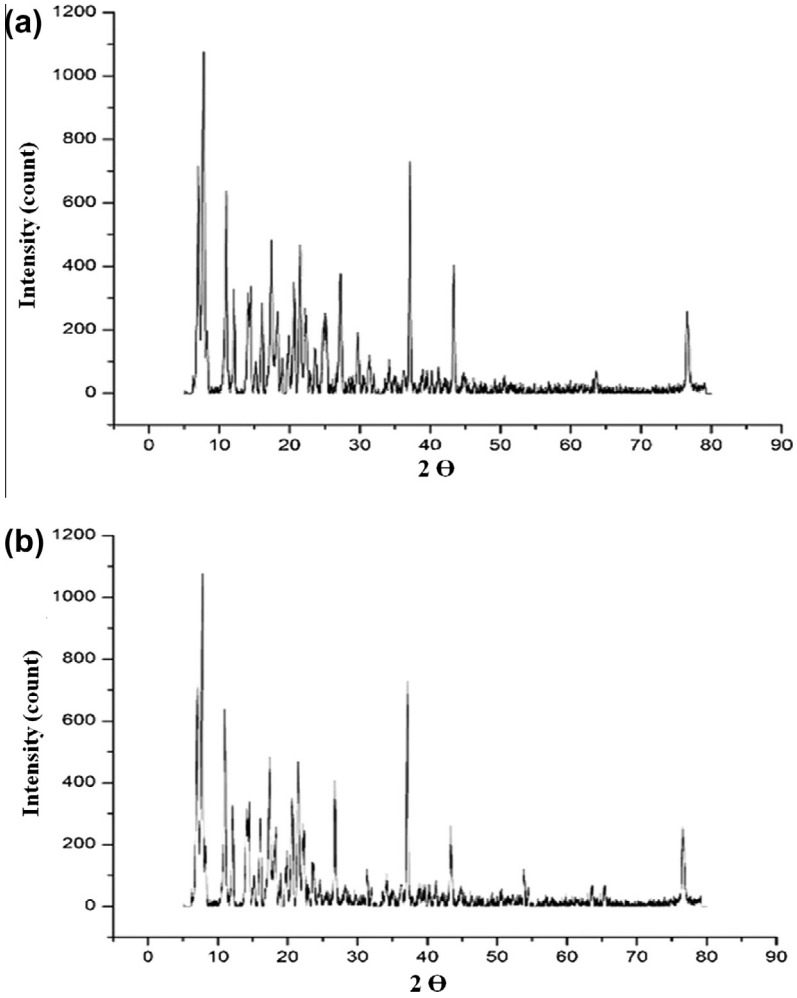

Fig. 2. The XRPD diffractograms of complexes (a) **1** and (b) **2** showing peaks at different scattering angles.

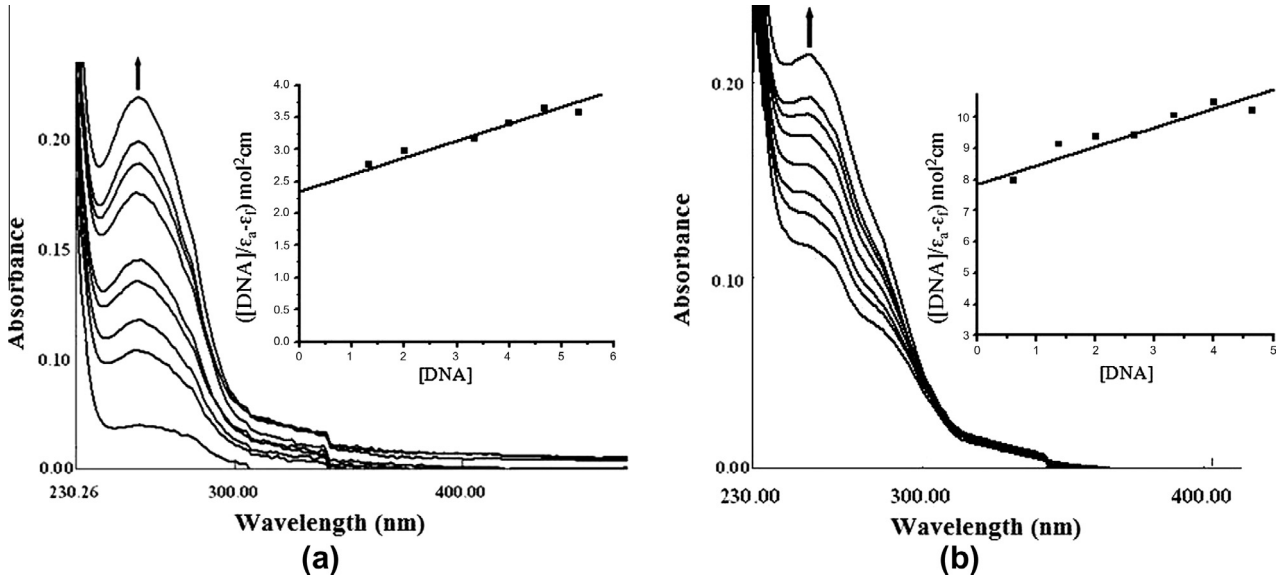

Fig. 3. Absorption spectral traces of complex (a) **1** and (b) **2** in 0.1 M Tris–HCl/10 M NaCl buffer at pH 7.2 upon the addition of CT DNA. Inset: plots of $[DNA]/\varepsilon_a-\varepsilon_f$ (m^2cm) vs. [DNA] for the titration of CT DNA with complexes ■, experimental data points; full lines, linear fitting of the data. [Complex] 10^{-5} M, [CT DNA] 0–4.66×10^{-5} M.

of the complexes **1** and **2** with CT DNA, the intrinsic binding constant (K_b) values of complexes **1** and **2** were calculated and are represented in Table 1. The high K_b value for **1** as compared to **2** is due to the fact that the latter has steric constraints caused

Table 1
The intrinsic binding constant (K_b), Scatchard binding constant (K) and Stern–Volmer quenching constant (K_{sv}) values of dipeptide complexes **1** and **2** with CT DNA (mean standard deviation).

Complex	K_b (M^{-1})	Monitored at (nm)	% Hyperchromism
1	4.3×10^4 (±0.14)	274	52
2	2.1×10^4 (±0.12)	273	38

by the bulky side chain of leucine containing methyl groups resulting in the relatively close stacking between the complex and the DNA base pairs accounting for its lower binding propensity with DNA.

3.2.2. Fluorescence titrations

The complexes **1** and **2** emit weak luminescence in Tris–HCl buffer at ambient temperatures with a maxima appearing at 390 nm when excited at 260 nm. The fluorescence emission titration of the complexes **1** and **2** were carried out with CT DNA under identical experimental conditions. Upon the addition of CT DNA the emission intensity of complexes **1** and **2** increased with no apparent change in the shape and position of the emission bands (Fig. 4). The hydrophobic molecular structure of CT DNA could be responsible for enhancing the fluorescence quantum yield of complexes, leading to the higher fluorescence intensity with the increase in concentration of the CT DNA [34]. The binding constant, K values of the complexes **1** and **2** were calculated and are represented in Table 2 which were in good agreement with the intrinsic binding constants as determined by UV–vis titrations.

3.2.3. Ethidium bromide displacement assay

To further investigate the mode of binding of the complexes **1** and **2**, the ethidium bromide (EB) displacement assay was carried out. On addition of complexes **1** and **2**, to CT DNA pretreated with EB, a decrease in emission intensity was observed. The emission intensity in absence and presence of **1** and **2** with EB–DNA are depicted in Fig. 5. As there is incomplete quenching of the EB-induced emission intensity, the intercalative binding mode for complexes was ruled out. Further, the quenching constants of complex **1** and **2** were quantitatively evaluated by Stern–Volmer equation and the K_{sv} values are represented in Table 2.

Table 2
The Scatchard binding constant (K) and Stern–Volmer quenching constant (K_{sv}) values of dipeptide complexes **1** and **2** with CT DNA (mean standard deviation).

Complex	K	Monitored at (nm)	K_{sv}
1	5.1×10^4 (±0.15)	390	2.60 (±0.09)
2	3.4×10^4 (±0.13)	390	1.92 (±0.08)

3.2.4. Circular dichroism

Circular dichroism is a useful technique to assess whether nucleic acids undergo conformational changes as a result of complex formation or changes in the environment. A solution of CT DNA exhibits a positive band (275 nm) from base stacking interactions and a negative band (245 nm) from the right-handed helicity of DNA. The CD spectrum of DNA exhibited change in both positive and negative bands when the dipeptide complexes **1** and **2** were incubated with CT DNA (Fig. 6). The complexes **1** and **2** exhibited an increase in intensities of negative (ellipticity) while a decrease in intensities of positive (helicity) bands revealing the binding of complexes *via* non-intercalative mode of binding i.e. groove binding. The decrease in the positive band by these complexes suggested that the complexes could unwind the DNA helix and lead to loss of helicity [35] and also that upon the interaction with the complexes **1** and **2**, the B-DNA transforms into an A-like conformation [36].

3.3. DNA cleavage activity

Besides the above methods, interactions between the Zn(II)-dipeptide complexes and DNA were also investigated by the cleavage assay of supercoiled pBr322 plasmid DNA. By incorporating both the metal sites and peptide-based DNA binding elements into a designed artificial nuclease, hydrolytically active metal ions may be positioned such to be capable of cleaving DNA backbone [37]. The cleavage of the plasmid DNA was analyzed by monitoring the conversion of supercoiled circular DNA (Form I) to nicked DNA (Form II) and/or linear DNA (Form III).

Firstly, a concentration dependent DNA cleavage by the complex **1** was performed. Fig. 7a shows that Form I plasmid DNA is gradually converted into Form II without the formation of Form III, suggesting single strand DNA cleavage by complex **1**.

The nuclease efficiency of the metal complexes is known to depend on the activators used for initiating the DNA cleavage [38].

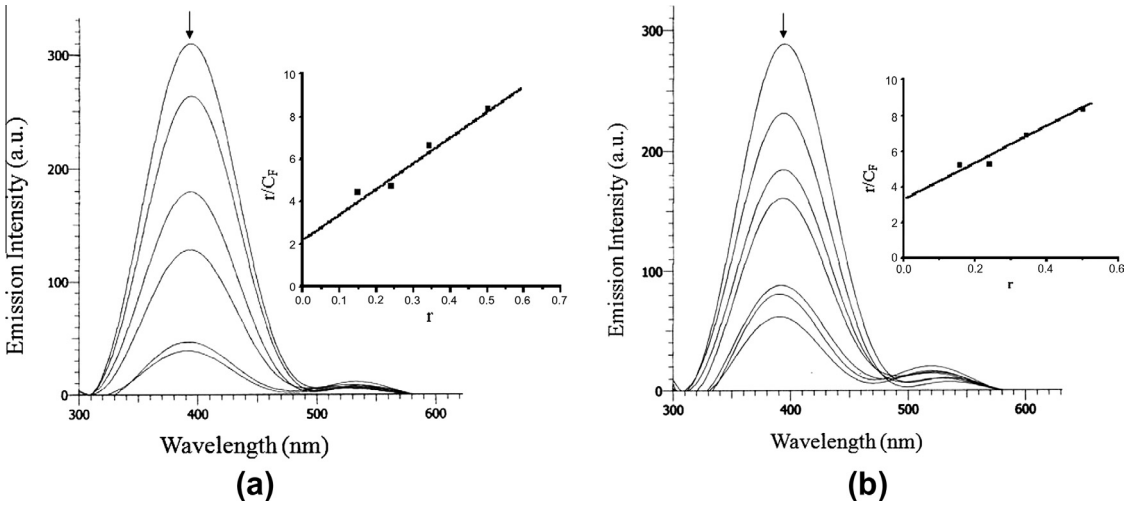

Fig. 4. Emission spectra of the complex (a) **1** and (b) **2** with increasing concentration of complexes in the absence and presence of CT DNA in Tris HCl buffer (pH 7.2). Arrows indicate change in intensity upon increasing concentration of CT DNA. Inset: Plots of r vs. r/C_F for the titration of CT DNA with complexes. [Complex] 6.66×10^{-6} M, [CT DNA] $0.66–4.0 \times 10^{-6}$ M.

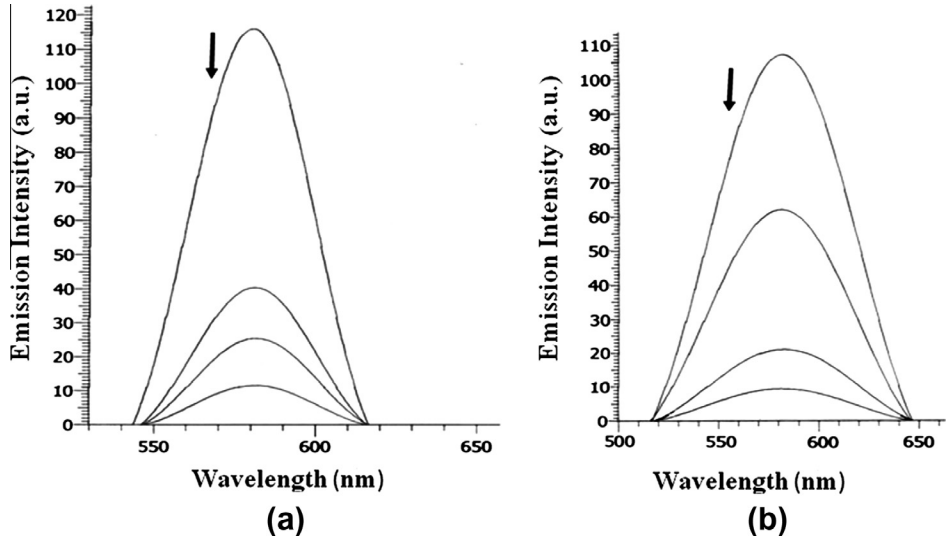

Fig. 5. Emission enhancement spectra of the complexes (a) **1** and (b) **2** with increasing concentration of complexes in presence of fixed concentration of EB–DNA in Tris HCl buffer (0.01 M, pH 7.2). Arrow indicates change in intensity upon increasing concentration of complexes. [Complex] 0.66–4.66 × 10^{-5} M, [EB–DNA] 0.66 × 10^{-6} M.

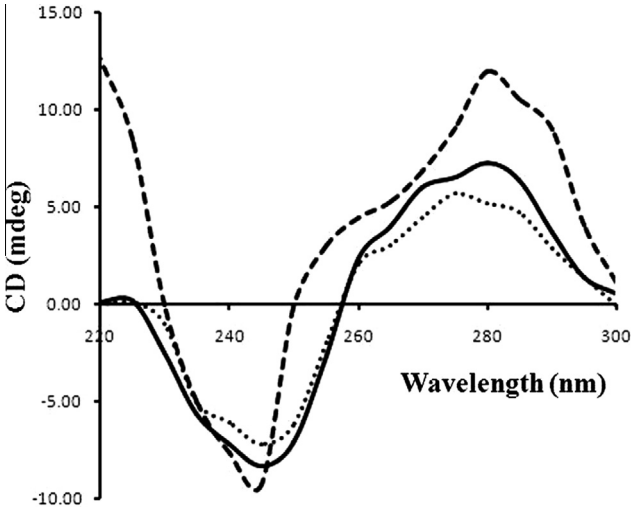

Fig. 6. CD spectra of CT DNA alone (————), in presence of complex **1** (……) and in presence of complex **2** (––––). [Complex] 10^{-3} M, [CT DNA] 10^{-3} M.

The DNA cleavage activity of complex **1** in presence of H_2O_2, 3-mercaptopropionic acid (MPA), ascorbate (Asc) and glutathione (GSH) was evaluated and the cleavage activity of complex **1** was significantly enhanced by these activators where the activity followed the order MPA >> H_2O_2 > Asc ≈ GSH (Fig. 7b, Lanes 2–5).

The DNA cleavage mechanism by complex **1** was primarily investigated in the presence of reactive oxygen species *viz.*, hydroxyl radical scavengers (DMSO and EtOH), singlet oxygen quencher (NaN_3) and SOD as superoxide radical scavenger under identical conditions. These species contain a photo or a redox active center, which causes damage to the sugar and/or base [39]. As depicted in Fig. 7b, insignificant inhibitions were observed in the presence of DMSO and EtOH (Lanes 8 and 9), ruling out the possibility of DNA cleavage by a hydroxyl radical. While, on the other hand, addition of NaN_3 (Lane 6) did not show any significant effect on the DNA strand scission indicative of non-involvement of singlet oxygen for DNA cleavage. However, superoxide dismutase SOD (Lane 7) enhances the cleavage efficiency. This indicates that the cleavage of DNA probably follows a discernable hydrolytic cleavage mechanism.

To clarify the aspects of the mechanism, groove binders such as DAPI (minor groove binder) and methyl green (major groove binder) were used. As the dimensions of the two grooves are different, targeting them requires vastly dissimilar and different shaped molecules. The addition of DNA cleavage was inhibited in the presence of DAPI (Lane 2) suggesting the minor groove to be the preferred interacting site of complex **1** (Fig. 7c). In general, Cu(II) complexes typically bind GC regions of DNA by intercalation, but associate in the grooves in AT regions [40], whereas, complexes with hexadentate ions such as zinc(II), bind primarily to AT regions, in a non-intercalative manner [41]. It is clear that metal complexes offer great potential as structure-selective binding agents for nucleic

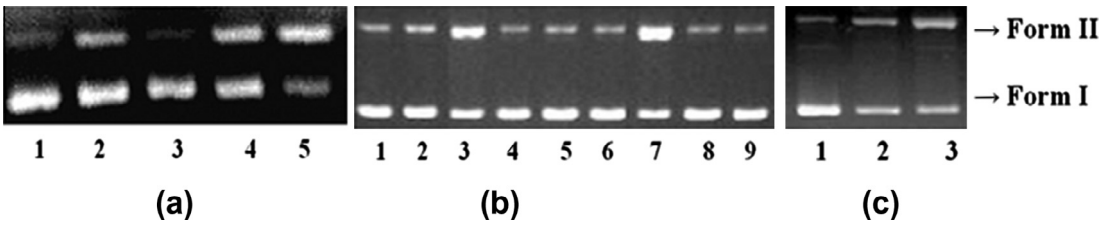

Fig. 7. The cleavage patterns of the agarose gel electrophoresis diagram showing cleavage of pBR322 supercoiled DNA (300 ng) by complex **1** at 310 K after 45 min of incubation; (a) Lane 1, DNA control; Lane 2, 10 μM of complex + DNA; Lane 3: 20 μM of complex + DNA; Lane 4: 30 μM of complex + DNA; Lane 5: 40 μM of complex + DNA, (b) in presence of different activating agents. Lane 1: DNA Control; Lane 2: 40 μM of complex + H_2O_2 (0.4 M) + DNA; Lane 3: 40 μM of complex + MPA (0.4 M) + DNA; Lane 4: 40 μM of complex + ASc (0.4 M) + DNA; Lane 5: 40 μM of complex + GSH (0.4 M) + DNA; Lane 6: 40 μM of complex + NaN_3 (0.4 M) + DNA; Lane 7: 40 μM of complex + SOD (15 units) + DNA; Lane 8: 40 μM of complex + DMSO (0.4 M) + DNA; Lane 9: 40 μM of complex + EtOH (0.4 M) + DNA and (c) in presence of DNA recognition agents. Lane 1, DNA control; Lane 2, 40 μM of complex + DNA + DAPI (8 μM); Lane 3, 40 μM of complex + DNA + methyl green (2.5 μL of a 0.01 mg/ml solution).

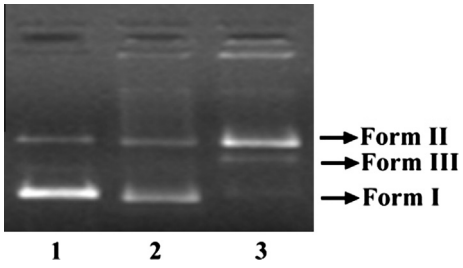

Fig. 8. Agarose gel electrophoresis pattern for the ligation pBR322 plasmid DNA linearized by complex **1**: Lane 1: DNA control; Lane 2: pBR322 plasmid DNA cleaved by complex **1**; Lane 3: ligation of linearized pBR322 plasmid DNA by T4 DNA ligase.

acids. Incorporation of hydrogen-bond donors and acceptors and/or van der Waals interaction recognition groups into metal complexes may allow the extremely high selectivity required for the metal complex to selectively bind a single nucleic acid site within a cell.

3.4. T4 DNA ligase assay

Since, the DNA cleavage mechanism by complex **1** was demonstrated to be hydrolytic in nature, we further investigated whether this cleavage is completely proceeding *via* the same hydrolytic mechanism as it is well documented for the DNA cleavage by restriction enzymes. We performed DNA religation experiments in which supercoiled pBR322 DNA was treated with T4 DNA ligase enzyme and subjected to gel electrophoresis (Fig. 8). It is well known that in DNA hydrolytic cleavage, the 3′-OH and 5′-OPO_3 (5′-OH and 3′-phosphate) fragments can be enzymatically ligated [42]. The complex **1** yielded linearized DNA which was religated by using T4 DNA ligase enzyme. The result after electrophoresis shows that the linear DNA fragments cleaved by the complex **1** can be religated by T4 DNA ligase enzyme.

3.5. Molecular docking studies

Molecular docking technique was further employed to understand the interaction mode between complex **1** and DNA double helix mainly in a non-covalent fashion [43]. The predicted top-ranking pose with the lowest energy of complex **1** was applied to predict the most stable and favorable orientation of complex inside the DNA double helix, and the highest binding affinity to DNA. As shown in Fig. 9, the complex reasonably binds with DNA sequence d(ACCGACGTCGGT)$_2$. The minimum energy docked structure obtained, suggests the best possible conformation of the Zn(II)-peptide complex interaction which is located within the central A–T (∼10.8 Å) rich regions of DNA in the minor groove as compared to peripheral G–C (∼13.2 Å) ones, due to enantioselectivity and site-specificity of Zn(II) complexes towards A–T region and leads to van der Waals interaction and hydrophobic contacts with DNA functional groups which define the stability of groove. In general, the deeper and narrower minor groove of AT-rich sequences, and the absence of the protruding 2-amino group of guanine (G), is optimal for accommodating the shape of the compound and for maximizing the stabilized van der Waal's contacts. Hydrogen bonding between the groove floor base pairs and the linking amides and electrostatic stabilizing interactions with the protonated amines are primary contributors to the overall ligand–DNA stability [44]. The proline ring of the Zn(II)-dipeptide complex **1** is arranged in a parallel fashion with respect to the deoxyribose groove walls of the DNA and was stabilized by hydrogen bonding between NH_2 of glycine moiety and C-2 carbonyl oxygen of T8.

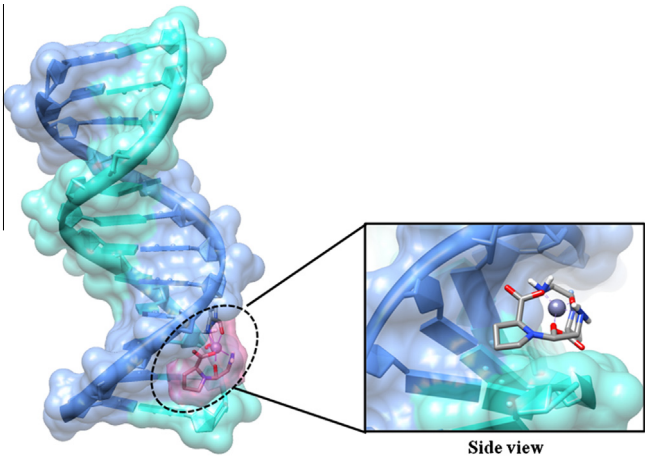

Fig. 9. Molecular docked model of the most favorable binding site of complex **1** with DNA dodecamer duplex of sequence d(CGCGAATTCGCG)$_2$ (PDB ID: 1BNA).

The resulting relative binding energy of docked complex **1** DNA was found to be −196.72 kJ mol^{-1}. This value is consistent with the spectroscopic binding studies. Drugs such as netropsin and distamycin bind to the minor grooves of DNA having AT-rich sequences [45].

4. Conclusions

Zn(II) complexes of dipeptide ligands (Pro-Gly/Pro-Leu) were synthesised and well-characterized by various spectroscopic data and elemental analysis. Their *in vitro* DNA binding interactions with CT DNA were studied by UV absorption, fluorescence spectroscopy and CD measurements. The results indicated that both the complexes **1** and **2** bind to the DNA preferentially *via* groove binding mode. The complex **1** was capable of cleaving the plasmid pBR322 DNA efficiently *via* hydrolytic pathway mechanism; validation was provided by T4 DNA ligase assay. Moreover, complex **1** inhibited DNA cleavage in presence of DAPI, suggesting the binding in the minor groove of the DNA helix. These studies were validated by molecular docking experiments of complex **1** with DNA, suggesting the binding of the complex **1** in the minor groove of DNA having AT-rich sequences. Our findings may give a new application and open a new way in the design of more effective and useful peptide-based complexes for DNA hydrolysis.

5. Abbreviations

EDCI	1-Ethyl-3-(3-dimethylaminopropyl)carbodiimide hydrochloride
HOBT	N-hydroxybenzotriazole
UV–vis	UV–visible
CT DNA	Calf thymus DNA
Tris	Tris(hydroxymethyl)aminomethane
EB	Ethidium bromide
CD	Circular dichroism

Acknowledgements

The authors are grateful to *RSIC*, CDRI, Lucknow; *SAIF*, Panjab University, Chandigarh; *STIC*, Cochin University, Cochin; *AIRF*,

JNU, Delhi, Center of Excellence in Material Science (Nanomaterial), AMU, Aligarh, India for providing ESI–MS, NMR, elemental analysis, CD and XRPD facility, respectively.

References

[1] E.L. Hegg, J.N. Burstyn, Toward the development of metal–based synthetic nucleases and peptidases: a rationale and progress report in applying the principles of coordination chemistry, Coord. Chem. Rev. 173 (1998) 133–165.

[2] T. Helleday, E. Petermann, C. Lundin, B. Hodgson, R.A. Sharma, DNA repair pathways as targets for cancer therapy, Nat. Rev. Cancer 8 (2008) 193–204.

[3] C.Y. Zhou, X.L. Xi, P. Yang, Studies on DNA binding to metal complexes of Sal_2trien, Biochemistry (Moscow) 72 (2007) 37–43.

[4] R. Ren, P. Yang, W. Zheng, Z. Hua, A simple copper(II)-L-histidine system for efficient hydrolytic cleavage of DNA, Inorg. Chem. 39 (2000) 5454–5463.

[5] J.C. Mai, Z. Mi, S-H Kim, B. Ng, P.D. Robbins, A Proapoptotic peptide for the treatment of solid tumors, Cancer Res. 61 (2001) 7709–7712.

[6] R.A. Cruciani, J.L. Barker, M. Zasloff, H.C. Chen, O. Colamonici, Antibiotic magainins exert cytolytic activity against transformed cell lines through channel formation, Proc. Natl. Acad. Sci. USA 88 (1991) 3792–3796.

[7] S.A. Johnstone, K. Gelmon, L.D. Mayer, R.E. Hancock, M.B. Bally, In vitro characterization of the anticancer activity of membrane-active cationic peptides. I. Peptide-mediated cytotoxicity and peptide-enhanced cytotoxic activity of doxorubicin against wild-type and p-glycoprotein over-expressing tumor cell lines, Anti-Cancer Drug Des. 15 (2000) 151–160.

[8] F.J. Sharom, G. DiDiodota, X. Yu, K.J.D. Ashbourne, Interaction of the P-glycoprotein multidrug transporter with peptides and ionophores, J. Biol. Chem. 270 (1995) 10334–10341.

[9] F. Huber, R. Barbieri, in: B.K. Keppler (Ed.), Metal complexes in cancer chemotherapy, VCH, Weinheim, 1993, pp. 353–368.

[10] N.Y. Sardesai, K. Zimmermann, J.K. Barton, DNA recognition by peptide complexes of rhodium(III): example of a glutamate switch, J. Am. Chem. Soc. 116 (1994) 7502–7508.

[11] F. Arjmand, S. Parveen, D.K. Mohapatra, Synthesis, characterization of Cu(II) and Zn(II) complexes of prolinecglycine and proline–leucine tetrapeptides: *In vitro* DNA binding and cleavage studies, Inorg. Chim. Acta 388 (2012) 1–10.

[12] P.R. Reddy, S.K. Mohan, K.S. Rao, Ternary zinc(II)-dipeptide complexes for the hydrolytic cleavage of DNA at physiological pH, Chem. Biodiver. 2 (2005) 672–682.

[13] J. Marmur, A procedure for the isolation of deoxyribonucleic acid from micro-organisms, J. Mol. Biol. 3 (1961) 208–214.

[14] M.E. Reicmann, S.A. Rice, C.A. Thomas, P. Doty, A further examination of the molecular weight and size of desoxypentose nucleic acid, J. Am. Chem. Soc. 76 (1954) 3047–3053.

[15] A. Wolfe, G.H. Shimer, T. Meehan, Polycyclic aromatic hydrocarbons physically intercalate into duplex regions of denatured DNA, Biochemistry 26 (1987) 6392–6396.

[16] J.R. Lakowiez, G. Webber, Quenching of fluorescence by oxygen. Probe for structural fluctuations in macromolecules, Biochemistry 12 (1973) 4161–4170.

[17] F. Arjmand, S. Parveen, M. Afzal, M. Shahid, Synthesis, characterization, biological studies (DNA binding, cleavage, antibacterial and topoisomerase I) and molecular docking of copper(II) benzimidazole complexes, J. Photochem. Photobiol. B: Biol. 114 (2012) 15–26.

[18] F. Arjmand, S. Parveen, M. Afzal, L. Toupet, T.B. Hadda, Molecular drug design, synthesis and crystal structure determination of Cu^{II}–Sn^{IV} heterobimetallic core: DNA binding and cleavage studies, Eur. J. Med. Chem. 49 (2012) 141–150.

[19] D.W. Ritche, V. Venkataraman, Ultra-fast FFT protein docking on graphics processors, Bioinformatics 26 (2010) 2398–2405.

[20] M. Bodanszky, A. Bodanszky, The practice of peptide synthesis, Springer-Verlag, New York, 1984. 1–282.

[21] M. Nath, S. Pokharia, G. Eng, X. Song, A. Kumar, Comparative study of structure– activity relationship of di- and tri-organotin(IV) derivatives of amino acid and peptides, J. Organomet. Chem. 669 (2003) 109–123.

[22] E. Katsoulakou, M. Tiliakos, G. Papaefstathiou, A. Terzis, C. Raptopoulou, G. Geromichalos, K. Papazisis, R. Papi, A. Pantazaki, D. Kyriakidis, P. Cordopatis, E.M. Zoupa, Diorganotin(IV) complexes of dipeptides containing the α–aminoisobutyryl residue (Aib): preparation, structural characterization, antibacterial and antiproliferative activities of [(n-Bu)2Sn(H-1L)] (LH = H–Aib–L–Leu–OH, H-Aib–L–Ala–OH), J. Inorg. Biochem. 102 (2008) 1397–1405.

[23] K. Nakamoto, Infrared and Raman Spectra of Inorganic and Coordination Compounds, fourth ed., Wiley, New York, 1986. pp. 233–244.

[24] M. Chauhan, K. Banerjee, F. Arjmand, DNA binding studies of novel copper(II) complexes containing L–tryptophan as chiral auxiliary: in vitro antitumor activity of Cu–Sn^2 complex in human neuroblastoma cells, Inorg. Chem. 46 (2007) 3072–3082.

[25] M. Nath, S. Pokharia, G. Eng, X. Song, A. Kumar, New triorganotin (IV) derivatives of dipeptides as models for metal–protein interactions: Synthesis, structural characterization and biological studies, Spectrochim. Acta A 63 (2006) 66–75.

[26] R.C. Maurya, D.D. Mishra, S. Mukherjee, J. Dubey, Metal cyanonitrosyl complexes: synthesis, magnetic and spectral studies of some novel mixed–ligand cyanonitrosyl $[CoNO]_{8-}$ complexes of cobalt(I) with heterocyclic bases, Polyhedron 14 (1995) 1351–1358.

[27] Y.-C. Lee, P.L. Jackson, M.J. Jablonsky, D.D. Muccio, R.R. Pfister, J.L. Haddox, C.I. Sommers, G.M. Anantharamaiah, M. Chaddha, NMR conformational analysis of cis and trans proline isomers in the neutrophil chemoattractant, N-acetyl-proline–glycine-proline, Biopolymers 58 (2001) 548–561.

[28] A. Patra, S. Sarkar, T. Mukherjee, E. Zangrando, P. Chattopadhyay, Zinc(II) complexes of 1,3-bis(2-pyridylmethylthio)propane: anion dependency, crystal structure and DNA binding study, Polyhedron 30 (2011) 2783–2789.

[29] J. Dehand, J. Jordanov, F. Keck, A. Mosset, J.J. Bonnet, J. Galy, Synthesis, crystal structure, and electronic properties of (L-methionylglycinato)copper(II), Inorg. Chem. 18 (1979) 1543–1549.

[30] C.Y. Zhou, J. Zhao, Y.B. Wu, C.X. Yin, P. Yang, Synthesis, characterization and studies on DNA-binding of a new Cu(II) complex with N1, N8–bis(l-methyl-4-nitropyrrole-2–carbonyl) triethylenetetramine, J. Inorg. Biochem. 101 (2007) 10–18.

[31] S. Rajalakshmi, T. Weyhermüller, A.J. Freddy, H.R. Vasanthi, B.U. Nair, Anomalous behavior of pentacoordinate copper complexes of dimethylphenanthroline and derivatives of terpyridine ligands: studies on DNA binding, cleavage and apoptotic activity, Eur. J. Med. Chem. 46 (2011) 608–617.

[32] A.A. Jain, M.R. Rajeshwari, Binding studies on peptide–oligonucleotide complex: intercalation of tryptophan in GC–rich region of c–myc gene, Biochim. Biophys. Acta 1622 (2003) 73–81.

[33] R. Nagane, T. Koshigoe, M. Chikira, Interaction of Cu(II)–Arg–Gly–His–Xaa metallopeptides with DNA: effect of C–terminal residues, leu and glu, J. Inorg. Biochem. 93 (2003) 204–212.

[34] S. Kashanian, M.B. Gholivand, F. Ahmadi, A. Taravati, A.H. Colagar, DNA interaction with Al–N, N′–bis(salicylidene)2,2′–phenylendiamine complex, Spectrochim. Acta Part A 67 (2007) 472–478.

[35] K. Karidi, A. Garoufis, N. Hadjiliadis, J. Reedijk, Solid-phase synthesis, characterization and DNA binding properties of the first chloro(polypyridyl)ruthenium conjugated peptide complex, Dalton Trans. (2005) 728–734.

[36] P. Lincoln, E. Tuite, B. Norden, Short–circuiting the molecular wire: cooperative binding of Δ–[Ru(phen)2d ppz]2+ and Δ–[Rh(phi)2bipy]3+ to DNA, J. Am. Chem. Soc. 119 (1997) 1454–1455.

[37] C. Liu, M. Wang, T. Zhang, H. Sun, DNA hydrolysis promoted by di- and multi-nuclear metal complexes, Coord. Chem. Rev. 248 (2004) 147–168.

[38] C.A. Detmer III, F.V. Pamatong, J.R. Bocarsly, Molecular recognition effects in metal complex mediated double-strand cleavage of DNA: reactivity and binding studies with model substrates, Inorg. Chem. 36 (1997) 3676–3682.

[39] J.-T. Wang, Q. Xia, X.-H. Zheng, H.-Y. Chen, H. Chao, Z.-W. Mao, L.-N. Ji, An effective approach to artificial nucleases using copper(II) complexes bearing nucleobases, Dalton Trans. 39 (2010) 2128–2136.

[40] F.R. Keene, J.A. Smith, J.G. Collins, Metal complexes as structure-selective binding agents for nucleic acids, Coord. Chem. Rev. 253 (2009) 2021–2035.

[41] E. Kikuta, M. Murata, N. Katsube, T. Koike, E. Kimura, Novel recognition of thymine base in double-stranded DNA by Zinc(II)-macrocyclic tetraamine complexes appended with aromatic groups, J. Am. Chem. Soc. 121 (1999) 5426–5436.

[42] M.E. Branum, A.K. Tipton, S. Zhu, L. Que Jr., Double-strand hydrolysis of plasmid DNA by dicerium complexes at 37 °C, J. Am. Chem. Soc. 123 (2001) 1898–1904.

[43] R. Rohs, I. Bloch, H. Sklenar, Z. Shakked, Molecular flexibility inab initio drug docking to DNA: binding-site and binding-mode transitions in all-atom Monte Carlo simulations, Nucl. Acids Res. 33 (2005) 7048–7057.

[44] R. Filosa, A. Peduto, S. Di Micco, P. de Caprariis, M. Festa, A. Petrella, G. Capranico, G. Bifulco, Molecular modelling studies, synthesis and biological activity of a series of novel bisnaphthalimides and their development as new DNA topoisomerase II inhibitors, Bioorg. Med. Chem. 17 (2009) 13–24.

[45] D.L. Boger, B.E. Fink, M.P. Hedrick, Total synthesis of distamycin A and 2640 analogues: a solution-phase combinatorial approach to the discovery of new, bioactive DNA binding agents and development of a rapid, high throughput screen for determining relative DNA binding affinity or DNA binding sequence selectivity, J. Am. Chem. Soc. 122 (2000) 6382–6394.